Some Steps towards Modelling of Dislocation Assisted Rafting: A Coupled 2D Phase Field – Continuum Dislocation Dynamics Approach

Ronghai Wu[1], Stefan Sandfeld[1]

[1]Institute of Materials Simulation (WW8), Department of Materials Science,
Friedrich-Alexander University of Erlangen-Nürnberg (FAU),
Dr.-Mack-Str. 77, 90762 Fürth, Germany

Keywords: Rafting, Phase field, Continuum dislocation dynamics, Nickel-based superalloy

Abstract

The interaction between edge dislocations and γ' precipitates as in nickel-based superalloys is studied by coupling a phase field model and a 2D continuum dislocation dynamic model. Various stresses, which serve as communicator between dislocations and precipitates, are calculated by an eigenstrain method for both the γ/γ' misfit and the dislocations. Our simulations show how edge dislocations tend to move to and pile up at specific γ/γ' interfaces. The growth of γ' is inhibited at the interface where dislocations are piling up, due to the reduction of elastic energy. The potential of our coupled model for simultaneous microstructure patterning and mechanical property prediction is discussed.

Introduction

Single crystal nickel-based superalloys have been widely used in e.g. turbine blades which operate under extreme conditions: temperatures are very high and are additionally accompanied by strong, sustaining centrifugal forces. One of the common approaches to assess the service performance and to understand the underlying mechanism is based on creep tests. Because in-situ observations of the (dislocation or γ') microstructure cannot easily be conducted, creep experiments usually have to be interrupted at specific representative stages at which then microstructural information can be conveniently obtained ex-situ. Additionally, creep tests are very time-consuming. Despite these two cumbersome aspects, a large amount of information about the deformation behavior and the microstructure of γ/γ' and dislocations have been gained in the past decades [1].
The above mentioned shortcomings strongly motivated the development of modeling and simulation methods for nickel-based superalloys. Phenomenological continuum models for elasto-plastic material behavior have been proposed within the framework of internal variables [2, 3]. Using e.g. the average dislocation density or the γ' size as internal variables one can well fit simulations results to experimental results, which makes these models useful as computational tools for roughly estimating service life and mechanical behavior. However, there is no general consensus regarding the choice of internal variables and detailed microstructural effects as e.g. the interaction between dislocations and precipitates are not directly accounted for in these models. However, it is well accepted

that dislocation associated interactions are one of the key underlying mechanisms during creep deformation: recent molecular dynamic (MD) and discrete dislocation dynamic (DDD) simulations revealed a number of details of the dislocation-precipitate interaction at the γ/γ' interface [4, 5]. For simplicity, in these simulations the γ/γ' microstructure is usually assumed to be static in time. Additionally, dislocation associated creep is a multi-time scale problem because the time-scale on which the γ/γ' evolution takes place is much larger than that of the dislocation flow, which makes the treatment very complicated and computationally expensive from a numerical point of view. However, the problem of multiple length scales becomes much simpler if mesoscale models are used for both the γ/γ' evolution and the plasticity. Pioneering work has been done by coupling phase field models (PFM) for the evolution of the phase microstructure with constitutive plasticity models. E.g. Finel and co-workers [6] coupled a PFM to a viscoplasticity model and successfully reproduced rafting patterns, although their model does not contain any information about dislocation microstructure. Wang and co-workers [7] coupled the Kim-Kim-Suzuki (KKS) model to a strain gradient-based plasticity/phase field model and obtained rafting patterns together with information about dislocations. Strain gradient plasticity methods in general, however, only account for geometrically necessary dislocations (GNDs) and cannot represent the flow of dislocations.
In the present work, we show an alternative approach for coupling a PFM and a continuum model of dislocation dynamics: our PFM has one composition field and is used to describe the evolution of the γ/γ' phase microstructure, while a 2D continuum dislocation dynamics (CDD) model is used to represent fluxes of positive and negative edge dislocations (from which GNDs and SSDs – statistically stored dislocations – could be computed) [8, 9]. We focus especially on the interaction mechanism between the γ' precipitate and dislocations.

Model formulation

The following mathematical conventions and symbols are used: non-bold letters denote scalar or scalar fields, bold letters denote vectors or higher order tensors, non-italics stand for constants or superscript, italics for variables. ∇ and ∇^2 are the spatial gradient operator and the Laplace operator, respectively. The inner product and the double contraction are written as e.g. $\mathbf{a} \cdot \mathbf{b}$ and $\mathbf{A} : \mathbf{B}$, respectively.

Phase field model

We consider a Ni-Al binary system with no distinction of γ' variants. A simple phase field model with normalized composition field c is sufficient in this case:

$$c = \frac{c' - c^{\mathrm{e}}_{\gamma}}{c^{\mathrm{e}}_{\gamma'} - c^{\mathrm{e}}_{\gamma}} \tag{1}$$

where c' is the real composition, c^{e}_{γ} and $c^{\mathrm{e}}_{\gamma'}$ are the equilibrium compositions of γ and γ', respectively. Therefore, $c = 0$ denotes the γ phase and $c = 1$ stands for the γ' phase. The total energy of the system is given in functional form:

$$F = \int_{\mathrm{V}} (f^{\mathrm{bulk}} + f^{\mathrm{grad}} + f^{\mathrm{el}})\,\mathrm{dV} \tag{2}$$

with the energy densities

$$f^{\text{bulk}} = \mathrm{f}_0 c^2(1-c^2), \qquad f^{\text{grad}} = \frac{\lambda}{2} \mid \nabla c \mid^2, \qquad f^{\text{el}} = \frac{1}{2}\boldsymbol{\sigma}^{\text{el}} : \boldsymbol{\epsilon}^{\text{el}} \tag{3}$$

where f_0 is the energy density scale determined by the bulk energy density barrier, λ is the gradient energy density coefficient determined by fitting the calculated interface energy to the experimentally obtained interface energy. The sum of bulk energy and gradient energy gives the calculated interface energy (or chemical energy). The stress $\boldsymbol{\sigma}^{\text{el}}$ and strain $\boldsymbol{\epsilon}^{\text{el}}$ are obtained from solving the mechanical equilibrium equation. We assume that mechanical equilibrium is always reached instantaneously and that body forces from e.g. gravitation etc can be neglected. With this the governing equations are given as

$$\nabla \cdot \boldsymbol{\sigma}^{\text{el}} = \mathbf{0}, \qquad \boldsymbol{\sigma}^{\text{el}} = \boldsymbol{C} : \boldsymbol{\epsilon}^{\text{el}}, \qquad \boldsymbol{\epsilon}^{\text{el}} = \boldsymbol{\epsilon} - (\beta\boldsymbol{\epsilon}^{\text{mis}} + \boldsymbol{\epsilon}^{\text{dis}}) \tag{4}$$

where $\boldsymbol{\epsilon}^{\text{el}}$ is obtained in a small strain context from the additive decomposition of the total strain $\boldsymbol{\epsilon}$ into the elastic and inelastic contributions. The latter can consist of eigenstrains caused by the γ/γ' misfit $\boldsymbol{\epsilon}^{\text{mis}}$ (which is a diagonal tensor), or from dislocations eigenstrains $\boldsymbol{\epsilon}^{\text{dis}}$ (which is an off-diagonal tensor). The interface interpolation function β and stiffness tensor $\boldsymbol{C}$ are given as:

$$\beta = c^3(10-15c+6c^2), \qquad \boldsymbol{C} = \frac{1}{2}(\mathbf{C}_{\gamma'} + \mathbf{C}_{\gamma}) + (\beta - \frac{1}{2})(\mathbf{C}_{\gamma'} - \mathbf{C}_{\gamma}), \tag{5}$$

where $\mathbf{C}_{\gamma'}$ and $\mathbf{C}_{\gamma}$ are the stiffness tensors of the γ' and γ phase, respectively. The interface interpolation function $\beta(c)$ is responsible for the elastic inhomogeneity (with $\beta(c)|_{c=0} = 0$ and $\beta(c)|_{c=1} = 1$). Furthermore, the derivatives $\beta'(c)|_{c=0,c=1} = 0$ and $\beta''(c)|_{c=0,c=1} = 0$ imply that γ and γ' are equilibrium phases from the point of view of elastic energy.
Finally, we assume that the evolution of the γ/γ' phase microstructure is governed by the Allen-Cahn equation:

$$\frac{\partial c}{\partial t} = \mathrm{M}_c \nabla^2 \frac{\delta F}{\delta c}, \tag{6}$$

where M_c governs the interface mobility.

Continuum dislocation dynamics for edge dislocations

We use a continuum dislocation dynamic model for edge dislocations, which is able to distinguish between positive and negative edge dislocation density, ρ^+ and ρ^-. The total density $\rho = \rho^+ + \rho^-$ and excess density $\kappa = \rho^+ - \rho^-$ are derived from that and may change in time. The more commonly used GND and SSD densities can be determined by $\rho^{\text{GND}} = |\kappa|$ and $\rho^{\text{SSD}} = \rho - \rho^{\text{GND}}$, respectively.
The initial density distribution is constructed by superposition of m bundles of dislocations. Each bundle of dislocations is assumed to have the shape of a Gaussian normal distribution with standard deviation σ. Using x_i' as the local coordinate of the ith dislocation bundle in glide direction (cf. Fig.1) the density is given by

$$\rho^{(+\text{or}-)}(x_i') = \frac{\mathrm{N}}{\mathrm{h}\sigma\sqrt{2}} \exp\left(-\frac{x_i'^2}{\sqrt{2}\sigma}\right), \tag{7}$$

where N is the number of discrete dislocations, and h is the height of slip lamella (i.e. averaging height for converting discrete dislocations into a density, see [8]). The initial

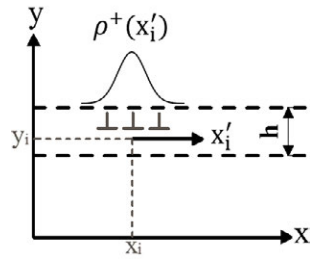

Figure 1: Schematic of the slip system geometry. Each density distribution is located at coordinate (x_i, y_i), which has Gaussian shape in x direction and is constant along the y direction within the averaging height h.

plastic slip distribution s depends on the Burgers vector $\mathbf{b}$ and the motion history (i.e. from which direction initial dislocations have moved into the domain), given by

$$s(x_i') = \begin{cases} \mathrm{sign}(\mathbf{b})\mathrm{b}\int_{x_i'}^{+\infty} \kappa(\tilde{x})\,\mathrm{d}\tilde{x} & \text{if } \rho^{(+\mathrm{or}-)} \text{ moved along positive } x_i' \text{ direction} \\ \mathrm{sign}(\mathbf{b})\mathrm{b}\int_{-\infty}^{x_i'} \kappa(\tilde{x})\,\mathrm{d}\tilde{x} & \text{if } \rho^{(+\mathrm{or}-)} \text{ moved along negative } x_i' \text{ direction} \end{cases} \tag{8}$$

where b is the magnitude of the Burgers vector, sign($\mathbf{b}$) gives the direction of $\mathbf{b}$ in this 1D setting. The resulting initial conditions of dislocation density and plastic slip s are simply the sum of all local fields.
The resulting stress and strain can be obtained by linking the plastic slip to a shear eigenstrain by

$$\boldsymbol{\epsilon}^{\mathrm{dis}} = s\mathbf{M} \qquad \text{with } \mathbf{M} = \frac{1}{2\mathrm{b}}(\mathbf{b}\otimes\mathbf{n} + \mathbf{b}\otimes\mathbf{n}). \tag{9}$$

For simplicity, we assume that neither annihilation nor multiplication take place (which in reality is of course only a rough approximation). The evolution equations for ρ^+, ρ^- and s are given by

$$\frac{\partial\rho^+}{\partial t} = -\partial_x(v\rho^+), \qquad \frac{\partial\rho^-}{\partial t} = \partial_x(v\rho^-), \qquad \frac{\partial s}{\partial t} = \rho v\mathrm{b}. \tag{10}$$

Assuming a linear relationship between stresses and dislocation velocity v, we can write the dislocation velocity law as

$$v = \begin{cases} \frac{\mathrm{b}}{\mathrm{B}}(\tau^{\mathrm{l}} + \tau^{\mathrm{b}} - \tau^{\mathrm{y}}) & \text{if } |\tau^{\mathrm{l}} + \tau^{\mathrm{b}}| > \tau^{\mathrm{y}}, \\ 0 & \text{else} \end{cases} \tag{11}$$

where B is the drag coefficient. τ^{l} is long-range shear stress field resulting from external loading, heterogeneous plastic strain and the γ/γ' misfit. After solving (4), τ^{l} is obtained as the shear component of $\boldsymbol{\sigma}^{\mathrm{el}}$. τ^{b} is the back stress and τ^{y} is the yield stress [10] given by

$$\tau^{\mathrm{b}} = -\mathrm{DGb}\frac{\partial_x\kappa}{\rho}, \qquad \tau^{y} = \frac{\alpha\mathrm{bG}\sqrt{\rho}}{1-\beta} \tag{12}$$

where G is the shear modulus, D $\in [0.6, 1]$ and $\alpha \in [0.2, 0.4]$ are two non-dimensional parameters. The factor $1/(1-\beta)$ in τ^y reflects the experimental observation that dislocations hardly move into γ': $\tau^y \to \infty$ inside the precipitate results in zero velocity, while outside the precipitate τ^y is just the commonly used Taylor-type yield stress, with a smooth transition in between.

Results and discussion

The anisotropy of γ/γ' is around 3, which gives a cubic morphology of γ'. Slip planes are oriented 45^0 to the γ/γ' interfaces. To make the numeric implementation easier, the whole sample is rotated by 45^0. After rotation, the slip system is parallel to the x-axis (see Fig.1) and the γ' shape becomes rhombic. We use periodic boundary conditions and only one representative γ' precipitate at the domain center. Without external loading and plasticity, the precipitate will keep growing in symmetrically rhombic shape until both γ and γ' are at equilibrium composition. To study the dislocation-precipitate interaction and the influence of external loading, we set up different dislocation initial conditions as described in the following two systems.

System 1

We prescribe a column of positive edge dislocations at the left side of the precipitate, as shown in Fig.2 (a) and (d). The morphology of the precipitate can be seen from the contour of the interfaces, because the driving force $M_c \nabla^2 \frac{\delta F}{\delta c}$ for the γ/γ' evolution vanishes inside pure γ and pure γ'. At the intermediate time step, positive edges dislocations move towards the right direction and pile up at the lower-left interface, while negative edge dislocations move to the left, as shown in Fig.2 (e). The reason is that τ^l resulting from the γ/γ' misfit is positive near the lower-left interface, whereas it is negative near the upper-right interface. Because of the dislocation pile-up, the eigenstrains (and thus the local stresses) resulting from the γ/γ' misfit are neutralized to some extend, therefore reducing the elastic energy density and the driving force for the γ' growth at the lower-left interface. The morphology symmetry is broken and the favorable growing direction shifts towards the upper-left direction, as shown in Fig.2 (b). At the quasi-steady state, dislocations are still pinned at the lower-left interface due to the infinite τ^y inside the precipitate, which now has an obvious elongation in diagonal direction, as shown in Fig.2 (c) and (f). A similar preferential dislocation pile-up and precipitate growth also would happen at the other interfaces as a result of dislocation-precipitate interaction (not shown in the present paper).

System 2

As a more realistic system, we define a random dislocation distribution as initial condition (see Fig.3 (a) and (d)). 10 simulations are done, each with and without external stress, and in a post-processing step we averaged over the dislocation density and composition field for visualization purposes. Creep tests are usually done in $\langle 01 \rangle$ direction, which results in a shear stress in $\langle 11 \rangle$ direction. Since only the shear stress is the driving force for the motion of dislocations, this is applied as external shear stress in the rotated

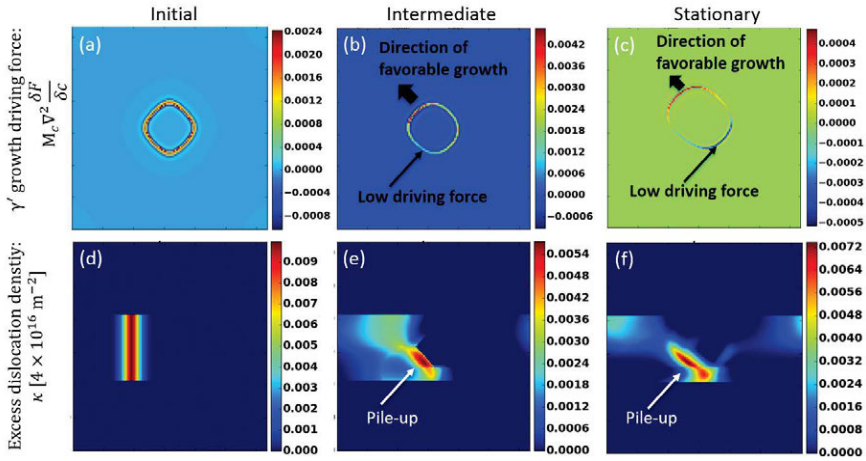

Figure 2: γ' growth driving force (upper row) and excess dislocation density (lower row): (a) and (d) initial condition, (b) and (e) intermediate step, (c) and (f) stationary state.

system. It can be seen that without external stress, the morphology of γ' is basically rhombic and symmetric (see Fig.3 (b) and (e)). The reason is that the dislocation influence on the γ' morphology is essentially determined by the relative dislocation density piling up at each interface and random initial dislocation distributions results in roughly equal amount of dislocation density piling at each interface. However, when there is an additional external loading, dislocations accumulate on average at the lower-left and upper-right interfaces (see Fig.3 (c) and (f)). Dislocation accumulations in the horizontal interfaces, which correspond to the lower-left and upper-right interfaces in the present rotated system, is widely observed in $\langle 10 \rangle$ direction creep tests. Due to the accumulation, the γ' coarsens in the diagonal direction (rafts), which is also widely observed in experiments and is a natural outcome of our model.

Existing MD or DDD simulations for nickel-based superalloys focus more on dislocation evolution, mesoscale PFM simulations more on γ/γ' patterning, while macroscale constitutive models concentrate on mechanical properties. Only few simulations can simultaneously deal with these three aspects. The present PFM-CDD coupled model already can handle dislocation glide and the γ/γ' evolution. Future work will extend the present simple model towards representing e.g. dislocation climb, annihilation and sources. Together with a CDD formulation that also is able to represent dislocations as curved and connected lines [11] this extended model could then reveal creep mechanisms that are of material scientific relevance and that may well predict the mechanical stress-strain behavior under creep conditions without any ad-hoc assumptions.

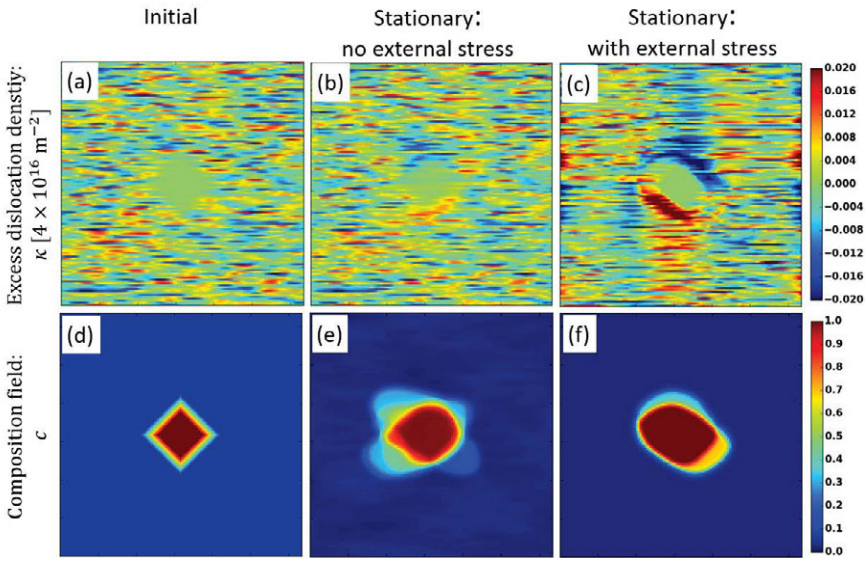

Figure 3: Excess density (top) and normalized composition (bottom) for ensemble averages of 10 systems with random initial dislocation distributions. From left to right: initial condition, stationary state without and with external stress.

Acknowledgements

S. S. gratefully acknowledges financial support from the Deutsche Forschungsgemeinschaft (DFG) through Research Unit FOR1650 'Dislocation-based Plasticity' (DFG grant Sa 2292/1-1).

References

[1] R. C. Reed, *The Superalloys: Fundamentals and Applications*. Cambridge University Press, 2006.

[2] M. F. Horstemeyer and D. J. Bammann, "Historical review of internal state variable theory for inelasticity," *International Journal of Plasticity*, vol. 26, pp. 1310–1334, 2010.

[3] J. Chaboche, "A review of some plasticity and viscoplasticity constitutive theories," *International Journal of Plasticity*, vol. 24, pp. 1642–1693, 2008.

[4] A. Prakash, J. Guenole, J. Wang, and J. Müller, "Atom probe informed simulations of dislocationprecipitate interactions reveal the importance of local interface curvature," *Acta Materialia*, vol. 92, pp. 33–45, 2015.

[5] S. Gao, M. Fivel, A. Ma, and A. Hartmaier, "Influence of misfit stresses on dislocation glide in single crystal superalloys: A three-dimensional discrete dislocation dynamics study," *Journal of the Mechanics and Physics of Solids*, vol. 76, pp. 276–290, 2015.

[6] A. Gaubert, Y. Le Bouar, and A. Finel, "Coupling phase field and viscoplasticity to study rafting in ni-based superalloys," *Philosophical Magazine*, vol. 90, pp. 375–404, 2010.

[7] N. Zhou, "Simulation study of directional coarsening (rafting) of γ' in single crystal Ni-Al," 2008.

[8] S. Sandfeld, M. Monavari, and M. Zaiser, "From systems of discrete dislocations to a continuous field description: stresses and averaging aspects," *Modelling and Simulation in Materials Science and Engineering*, vol. 21, pp. 1–22, 2013.

[9] M. Zaiser and S. Sandfeld, "Scaling properties of dislocation simulations in the similitude regime," *Modelling and Simulation in Materials Science and Engineering*, vol. 22, pp. 1–20, 2014.

[10] I. Groma, F. F. Csikor, and M. Zaiser, "Spatial correlations and higher-order gradient terms in a continuum description of dislocation dynamics," *Acta Materialia*, vol. 51, pp. 1271–1281, 2003.

[11] T. Hochrainer, S. Sandfeld, M. Zaiser, and P. Gumbsch, "Continuum dislocation dynamics: towards a physical theory of crystal plasticity," *Journal of the Mechanics and Physics of Solids*, vol. 63, pp. 167–168, 2014.